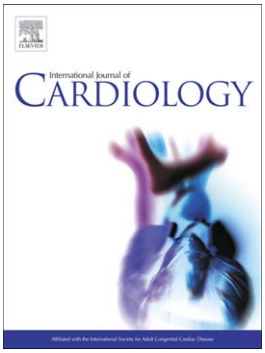

Synergistic impact of endurance training and intermittent hypobaric hypoxia on cardiac function and mitochondrial energetic and signaling

Magalhães J, Falcão-Pires I, Gonçalves IO, Lumini-Oliveira J, Marques-Aleixo I, dos Passos E, Rocha-Rodrigues S, Machado NG, Moreira AC, Miranda-Silva D, Moura C, Leite-Moreira AF, Oliveira PJ, TorrellaJR., Ascensão A

PII: S0167-5273(13)01526-X
DOI: doi: 10.1016/j.ijcard.2013.08.001
Reference: IJCA 16841

To appear in: *International Journal of Cardiology*

Received date: 3 June 2012
Revised date: 1 April 2013
Accepted date: 3 August 2013

Please cite this article as: J Magalhães, I Falcão-Pires, IO Gonçalves, J Lumini-Oliveira, I Marques-Aleixo, E dos Passos, S Rocha-Rodrigues, NG Machado, AC Moreira, D Miranda-Silva, C Moura, AF Leite-Moreira, PJ Oliveira, Torrella JR., A Ascensão, Synergistic impact of endurance training and intermittent hypobaric hypoxia on cardiac function and mitochondrial energetic and signaling, *International Journal of Cardiology* (2013), doi: 10.1016/j.ijcard.2013.08.001

Synergistic impact of endurance training and intermittent hypobaric hypoxia on cardiac function and mitochondrial energetic and signaling

Magalhães J[1*]✉, Falcão-Pires I[2], Gonçalves IO[1], Lumini-Oliveira J[1,3], Marques-Aleixo I[1], dos Passos E[1], Rocha-Rodrigues S[1], Machado NG[4], Moreira AC[4], Miranda-Silva D[2], Moura C[2], Leite-Moreira AF[2], Oliveira PJ[4], Torrella JR[5*], Ascensão A[1*]

[1]Research Centre in Physical Activity, Health and Leisure, Faculty of Sport, University of Porto, Portugal

[2]Department of Physiology and Cardiothoracic Surgery, Cardiovascular R&D Unit, Faculty of Medicine, University of Porto, Portugal

[3]Faculty of Health Sciences, University of Fernando Pessoa, Portugal

[4]Centre for Neurosciences and Cell Biology, Department of Life Sciences, University of Coimbra, Portugal

[5]Department of Physiology and Immunology, Faculty of Biology, University of Barcelona, Spain

* Contributed equally

✉ Corresponding author:

José Magalhães

Research Centre in Physical Activity, Health and Leisure

Faculty of Sport Sciences, University of Porto

Rua Dr. Plácido Costa, 91, 4200-450 Porto, Portugal

e-mail: jmaga@fade.up.pt

Running head: Endurance training and intermittent hypobaric hypoxia on cardiac function

Abstract

Background: Intermittent hypobaric-hypoxia (IHH) and endurance-training (ET) are cardioprotective strategies against stress-stimuli. Mitochondrial modulation appears to be an important step of the process. This study aimed to analyse whether a combination of these approaches provide additive or synergistic effects improving heart-mitochondrial and cardiac-function.

Methods: Two-sets of rats were divided into normoxic-sedentary (NS), normoxic-exercised (NE, 1h/d/5wks treadmill-running), hypoxic-sedentary (HS,6000m,5h/d/5wks) and hypoxic-exercised (HE) to study overall cardiac and mitochondrial function. *In vitro* cardiac mitochondrial oxygen consumption and transmembrane potential were evaluated. OXPHOS subunits and ANT protein content were semi-quantified by Western Blotting. HIF-1α, VEGF, VEGF-R1 VEGF-R2, BNP, SERCA2a and PLB expression were measured by qRT-PCR and cardiac function was characterized by echocardiography and hemodynamic parameters.

Results: Respiratory control ratio (RCR) increased in NE, HS and HE *vs.* NS. Susceptibility to anoxia/reoxygenation-induced dysfunction decreased in NE, HS and HE *vs.* NS. HS decreased mitochondrial complex-I and -II subunits; however HE completely reverted the decreased content in complex-II subunits. ANT increased in HE. HE presented normalized ventricular-arterial coupling (Ea), BNP myocardial levels and significantly improved myocardial performance as evaluated by increased cardiac output and normalization of the Tei index *vs.* HS.

Conclusion: Data demonstrates that IHH and ET confer cardiac mitochondria with a more resistant phenotype although without visible addictive effects at least under basal conditions. It is suggested that the combination of both strategies, although not additive, result into improved cardiac function.

Keywords: Physical exercise, altitude, cardioprotection, bioenergetics

Introduction

Several non-pharmacological approaches, including endurance training (ET) and intermittent hypobaric hypoxia (IHH) have been considered effective preventive strategies against cardiac and mitochondrial dysfunction caused by different stressors [1, 2]. Endurance training has been considered an effective trigger for protection against distinct cardiac pathophysiological events [3-5]. The activation of several signaling pathways and consequent metabolic and redox remodeling has been associated with a cardioprotective phenotype. ET-induced myocardial adaptations include induction of myocardial heat shock proteins, increased myocardial cyclooxygenase-2 activity, elevated endoplasmic reticulum stress proteins, nitric oxide production, improved function of sarcolemmal adenosine triphosphate (ATP)-sensitive potassium channels and increased myocardial antioxidant capacity [3]. In addition, the signaling and mechanical remodeling induced by ET also leads to alterations on mitochondrial physiology which contribute to the overall cardioprotective phenotype. Furthermore, despite some controversy [6], cardioprotection afforded by chronic exercise might also be mediated by activation of mitochondrial ATP-sensitive potassium channels (mitoKATP) [7].

On the other hand, published data suggest that cardiac tolerance to acute oxygen deprivation can also be prevented by previous long-term exposure to IHH associated with natural or simulated high altitude conditions. In fact, a significant amount of data [2, 8] showed that previous IHH decreases myocardial infarction size, reduces the number of ventricular arrhythmias, and improves the recovery of cardiac contractile function against acute ischemia-reperfusion (I/R) injury. Although the molecular mechanisms related with the cardioprotective effect of chronic IHH are not completely understood, a selection of putative candidates have been proposed including an increased generation of reactive oxygen species (ROS) [9], nitric oxide [10], and the up-regulation of protein kinase C-delta [9], which would serve to prime the tissue to better handle later deleterious stimuli. In addition, both the activation of the mitoKATP channels [11, 12]

and the increased tolerance of heart mitochondria to calcium-induced MPTP opening [13] seem to contribute to the cardioprotection provided by IHH against I/R injury. Therefore, both the cardioprotective phenotype provided by ET and IHH may share, at least in part, some common signaling pathways. Consequently, an important question is whether hearts submitted to intermittent hypoxia can be further primed with ET so that the protective phenotype is increased.

Our hypothesis for this work is that IHH exposure plus an ET regimen in an animal model act in an additive or synergistic manner to increase the putative protective adaptations in the heart, especially at the mitochondrial level. To answer our relevant experimental question, male rats were submitted to IHH and ET alone and sequentially and hemodynamic measurements before and after volume overload, as well as echocardiography were used to assess cardiac function. Moreover, mitochondrial bioenergetics and resistance to *in vitro* anoxia and reoxygenation were also determined.

Methods

Reagents

ECL-Plus was purchased from GE Healthcare UK (RPN2132) and PVDF-membrane from BIORAD-US (62-0182). OXPHOS cocktail antibodies were purchased from Mitosciences/Abcam-US (MS604), anti-SIRT3 antibody from Cell Signaling-US (2627S), anti-ANT antibody from Santa Cruz-US (Sc-9299), and secondary antibodies were purchased from GE Healthcare-UK (RPN2124) and from Jackson Immunoresearch-US (705-035, 111-035-003). Rat VEGF EIA Kit was purchased from R&D systems Europe (RRV00). All other chemicals were purchased from Sigma Aldrich (Portugal).

Animal Care and Treatment

Two sets of forty Wistar male rats (aged 5 weeks, weighting around 190 g at the beginning of the experiments) were randomly divided into four groups (n=10 per group): normoxic-sendentary (NS), normoxic-exercised (NE), hypoxic-sendentary (HS)

and hypoxic-exercised (HE). The first set of animals was used to study *in vitro* mitochondrial function and related molecular biology markers and the second to perform echocardiography and *in vivo* cardiac hemodynamic evaluation. During the experimental protocol, all animals were housed in collective cages (two animals per cage) and maintained in a room at normal atmosphere (21-22ºC; 50-60% humidity) in 12 h light/12 h dark cycles, receiving standard food chow (A04-SAFE, Scientific Animal Food and Engineering, Augy, *France*) and water *ad libitium*. The study was approved by the local Institutional Review Board and follows the Guidelines for Care and Use of Laboratory Animals in research advised by the Federation of European Laboratory Animal Science Associations (FELASA). Several authors are accredited by FELASA to perform animal experimentation.

Intermittent Hypobaric Hypoxia (IHH) and Endurance Training (ET) Regimens

Animals in the hypoxic groups (HS, HE) were submitted to an acclimatization period of 5 h per day during 7 days in a hypobaric chamber (following the first day of hypoxia exposure at 2,500 m, altitude was incremented by 500 m/day until a simulated altitude of 6,000 m i.e., 49.3 kPa was reached). After the hypoxic acclimatisation period, the animals were exposed to intermittent hypobaric hypoxia during 5 weeks (5 h per day i.e., from 7-12 a.m., 5 days per week) at a simulated atmospheric pressure equivalent to an altitude of 6000 m [adapted from 14]. The lag phase to reach the established simulated altitude and to return to sea level conditions corresponded to 12 min. After the hypoxic period, the HE group rested for four hours before initiating the endurance treadmill training (from 4-5 p.m.). Animals of the normoxic groups (NS, NE) were maintained at an atmospheric pressure of 101.3 kPa (760 mmHg) equivalent to sea level throughout the protocol.

In coordination with the hypoxic regimen schedule, the animals from the exercised groups (NE, HE) were adapted to the treadmill running during 7 days (following the first two days of exercise at 15 $m.min^{-1}$, speed was increased by 5 $m.min^{-1}$ until 25 $m.min^{-1}$

were reached). After the adaptation period, the endurance-trained animals ran 1 h per day during 5 weeks at a speed of 25 $m.min^{-1}$ (0% gradient), whereas the non-exercised animals (NS, HS) were placed on a non-moving treadmill to minimize handling and environmental stress. All the animals completed the entire training program, hypobaric hypoxia exposure or both interventions.

Blood Collection and Heart Harvesting for Mitochondrial Studies

Twenty-four hours after the last training session, the set of animals used to study *in vitro* mitochondrial function were anaesthetised with ketamine (75 $mg.kg^{-1}$) and xylazine (5 $mg.kg^{-1}$) and the abdominal cavity was opened to expose the inferior cava vein. A blood sample of 2 mL was collected in an EDTA-containing tube for the determination of haemoglobin concentration and haematocrit. After fast chest opening, rat hearts were rapidly excised, rinsed, carefully dried and weighed.

Isolation of Heart Mitochondria

Mitochondria were prepared using conventional methods of differential centrifugation as described [15]. Mitochondrial and homogenate protein contents were determined by the Biuret method calibrated with BSA [16]. All isolation procedures were performed at 0-4°C. Considering the relatively greater abundance of intermyofibrillar (IMF) (~80%) compared with subsarcolemmal (SS) (~20%) mitochondria within the cells, a potentially dominant role for the IMF subfraction vs. the SS subfraction when studying mitochondrial alterations is expected.

Mitochondrial Oxygen Consumption Assays

Mitochondrial oxygen consumption was measured polarographically, at 25°C, using a Biological Oxygen Monitor System (Hansatech Instruments) and a Clark-type oxygen electrode (Hansatech DW 1, Norfolk, UK). Reactions were performed in 0.75 mL closed, temperature-controlled and magnetically stirred glass chamber containing 0.5

mg of mitochondrial protein in a respiration buffer containing 65 mM KCl, 125 mM sucrose, 10 mM Tris, 20 mM EGTA, 2.5 mM KH_2PO_4, pH 7.4. After 1-min equilibration period, mitochondrial respiration was initiated by adding glutamate (10 mM) plus malate (5 mM) or succinate (10 mM) plus rotenone (4 mM). State 3 respiration was measured after adding 333 nmol ADP; state 4 was considered as the rate of oxygen after full ADP phosphorylation. The respiratory control ratio (RCR, state3/state 4) and the ADP/O ratio (nmol ADP phosphorylated by natom O consumed), were calculated according to Estabrook [17], using 474 natom $O.mL^{-1}$ as the value for oxygen solubility at 25°C in double distilled water.

To evaluate the mitochondrial response to *in vitro* anoxia/reoxygenation (A/R), anoxia was performed exhausting oxygen in the reaction chamber after stimulating mitochondrial respiration with the addition of two ADP pulses in glutamate (10 mM) and malate (5 mM) energized mitochondria. Energized cardiac mitochondria were stimulated with an initial 333 nmol ADP pulse to obtain pre-anoxia respiratory rates. The anaerobic conditions were reached in state 4 through the addition of a second ADP pulse (1 mM), with the total period of anoxia set to 1 min. Anoxia was followed by 4 min of *in vitro* reoxygenation by exposing the reaction medium containing the mitochondrial suspension to open air while stirring the suspension. The polarographic oxygraph chamber was then closed and respiratory activities were measured again after the addition of another 333 nmol ADP pulse.

Mitochondrial Membrane Potential Measurements

Mitochondrial transmembrane potential (Δψ) was monitored indirectly based on the activity of the lipophilic cation tetraphenylphosphonium (TPP^+), followed by a TPP^+ selective electrode prepared as previously described [18]. Reactions were carried out in 1 mL of reaction buffer containing 65 mM KCl, 125 mM sucrose, 10 mM Tris, 20 mM EGTA, 2.5 mM KH_2PO_4, pH 7.4, supplemented with 3 µM TPP^+ and 0.5 mg/mL of protein with the temperature maintained at 25°C. For measurements of Δψ with

complex I substrates, energization was carried out with 10 mM of glutamate and 5 mM of malate and ADP-induced phosphorylation was achieved by adding 444 µM ADP. For measurements of Δψ with complex II substrates, 10 mM succinate supplemented with 4 µM rotenone were added to the medium containing 3 mM TPP^+ and mitochondria. The lag phase, which reflects the time needed to phosphorylate the added ADP, was also measured for both substrates.

Western Blotting Assays

Protein expression was determined by Western-Blot, for that equal amounts of protein (50 µg) were denatured in sample loading buffer and separated by dodecyl sulphate-polyacrylamide gel electrophoresis (SDS/PAGE), followed by a transference to a nitrocellulose membrane (Hybond-ECL, Amersham Biosciences). After blotting, membranes were blocked with 5% (w/v) non-fat dried milk or BSA in a Tris-buffered saline with Tween 20 (TBST-T). The membranes were then incubated with anti-ANT (1:1000 dilution; goat polyclonal, Santa Cruz Biotechnology sc-9299) and anti-Sirt3 (1:1000 dilution; rabbit monoclonal, Cell Signalling 2627). Primary antibodies were diluted in TBS-T containing 1% of non-fat dried milk or BSA for 2 h at room temperature (22-25ºC). After the incubation period, membranes were washed three times and incubated for 2h with horseradish peroxidase-conjugated anti-goat for ANT (1:10,000; Jackson ImmunoResearch 705-035-003) or anti-rabbit for SIRT3 (1:10,000; Jackson ImmunoResearch 111-035-003). Immunoreactive bands were visualized using ECL® chemiluminescence reagents (Amersham Biosciences), according to the manufacturer's instructions, followed by exposure to X-ray films (Sigma Z370398). Films were then analysed with Quantity One Software (BioRad Laboratories), and resulting absorbance values were expressed as the percentage variation of the NS group values.

The OXPHOS Western blotting kit (Mitosciences) containing a cocktail of monoclonal antibodies was used to semiquantify the relative levels of the subunits of the

mitochondrial oxidative phosphorylation NDUFB8 20 kDa of complex I, Fe-S 30 kDa-complex II, core 2 – 47 kDa of complex III and alpha 53 kDa subunit of ATP synthase. For detection of OXPHOS subunits, all previous steps were followed with exception of the following: after electrophoresis, proteins were electrophoretically transfered to polyvinylidene fluoride (Immobilon PVDF Transfer Membranes, Millipore) membranes and blocked with 5% (w/v) BSA in a TBST-T solution for 2 h at room temperature. Primary antibody against OXPHOS subunits (mouse monoclonal, MitoSciences MS604) were diluted in TBS-T (1:1,000 dilution) containing 1% of BSA and incubated overnight (4°C). Following antibody incubation and washing, membranes were incubated for 2 h at room temperature with an alkaline phosphatase-linked secondary antibody (goat anti-mouse; Jackson ImmunoResearch 115-055-174) diluted in TBS-T (1:2,500 dilution) containing 0.5% of BSA. The bands corresponding to the target proteins were detected and quantified using the ECF system (GE Healthcare) on the BioSpectrum Imaging System (Ultra-Violet Products). Equal protein transfer efficiency was verified by staining membranes with Ponceau S.

Echocardiography Assessment

Echocardiographic evaluation was performed immediately before the end of the experimental protocol, two days before hemodynamic evaluation, using a 7.5 MHz transducer. Animals were anaesthetized with ketamine (75 $mg.kg^{-1}$) and xylazine (5 $mg.kg^{-1}$) and allowed to stabilize for 15 min. All images were acquired in regular sinus rhythm, at a sweep speed of 200 mm/sec and stored in the system for off-line analysis (EchoPAC work station version 3.2 system, VingMed Ultrasound, GE). The assessment by M-mode guided by two-dimensional image performed in the left parasternal projection, using the short axis of the ventricles (LV), allowed to evaluate LV systolic function. This approach determined the measurement of the interventricular septum thickness (LV-IVS, mm), LV internal diameter (LV-ID, mm) and the posterior

wall thickness (LV-PW, mm) in diastole (d) and systole (s). Fractional shortening was calculated from measurements for the LV-ID in systole and diastole: FS (%)=[(LV-IDd–LVIDs)/LV-IDd]x100. LV ejection fraction was calculated using the cube method: EF (%)=[(LV-IDd^3–LVIDs^3)/LV-IDd^3]x100. The mitral E- and A-wave velocities were recorded via pulsed wave Doppler from the left parasternal apical 4-chamber view. Longitudinal velocities within the myocardium were recorded with pulsed-Tissue Doppler Imaging (TDI) from the apical 4-chamber window. The sample volume was placed within a myocardial segment and the spectral recording of velocities within the segment obtained, including peak myocardial systolic velocity (Sm, mm.s^{-1}), peak myocardial early diastolic velocity (Em, mm.s^{-1}) and peak myocardial late diastolic velocity (Am, mm.s^{-1}). As recommended, the sample volume was placed at the junction of the ventricular wall and mitral annulus.

Recordings were made at the interventricular septum and in the LV posterior wall. The myocardial performance (Tei) index of the LV was calculated according to the equation (a-b)/b, in which the “a” value equals the sum of isovolumic contraction time (IVCT, ms), ejection time (ms), and isovolumic relaxation time (IVRT, ms) and the “b” value equals the ventricular ejection time.

Cardiac Hemodynamic Measurements

Instrumentation: rats were anaesthetized by inhalation with a mixture of 4% sevoflurane with oxygen, intubated for mechanical ventilation (respiratory frequency 100 min and weight-adjusted tidal volume; Harvard Small Animal Ventilator - Model 683) and placed over a heating pad (37ºC). The ventilator setting and level of anaesthesia were adjusted to maintain the animal in an anesthetized state without spontaneous breathing efforts. The right jugular vein was cannulated for fluid administration (pre-warmed 0.9% NaCl solution) to compensate for perioperative fluid losses. A median sternotomy was performed to expose the heart and the pericardium was widely opened. Pressure-volume (PV) catheters were positioned along the long

axes of the left ventricle (LV) and right ventricle (RV) (PVR-1035, 1F, and PVR-1045, 1F, Millar Instruments, Houston, TX, respectively). The catheter was connected to MVP-300 conductance system (Millar Instruments), coupled to PowerLab16/30 converter (AD Instruments) and a personal computer for data acquisitions. Parameters from conductance catheter were recorded at a sampling rate of 1000 Hz in order to accurately capture all of the features of the pressure-volume waveforms produced by the fast beating rat hearts. Data were stored and analyzed with Millar conductance data acquisition and analysis software (PVAN3.5). A flow probe (200-367, Triton Technology, San Diego, CA) was positioned around the ascending aorta allowing cardiac output (CO) measurement with an ultrasonic flowmeter (Active Redirection Transit Time Flowmeter, System 6, Triton Technology, San Diego, CA). After complete instrumentation, the animal preparation was allowed to stabilize for 15 min. Hemodynamic recordings were made with respiration suspended at the end of expiration under steady-state conditions or during preload reductions (vena cava occlusions).

Measured parameters: Heart rate, stroke volume (SV, μl), cardiac output (CO, $mL.min^{1}$), ejection-fraction (EF, %), end-diastolic pressure (LV-EDP and RV-EDP, mmHg) and end-systolic pressure (LV-ESP and RV-ESP, mmHg) were determined from the LV pressure tracings. Effective systemic arterial elastance (E_A, $mmHg.\mu L^{-1}$), as a measure of LV afterload, was calculated dividing LV-ESP by the stroke volume. Relaxation rate was estimated with the time constant τ (ms) using the Glantz method.

The intrinsic myocardial function relatively load-independent parameters LV end-systolic pressure-volume relation (ESPVR, $mmHg.\ \mu L^{-1}$), preload recruitable stroke work (PRSW) and end-diastolic pressure-volume relation (EDPVR, $mmHg.\ \mu L^{-1}$) were determined from pressure-volume loops recorded during transient occlusion of the inferior vena cava by external progressive compression of the vessel. In order to assess inotropic reserve and evaluate cardiac response to acute stress conditions,

aortic occlusions were performed by abrupt narrowing or occlusion of the ascending aorta (AA) during the diastole, separating two heartbeats (isovolumic heartbeat). Increase in peak systolic pressure induced by AA occlusions was expressed as a percentage of peak systolic pressure of corresponding baseline heartbeats.

Parallel conductance values were obtained by the injection of approximately 20-30 μl of 10% NaCl into the right atrium. At the end of the experiment, the animals were sacrificed under anaesthesia and mechanical ventilation to obtain a terminal blood draw, and the heart was excised and snap-frozen in liquid nitrogen.

Plasma VEGF Content

In the set of animals used to study *in vivo* cardiac function, venous blood samples were collected in ethylenediamine-tetra-acetic acid-containing tubes, centrifuged at 5000 rpm for 15 min at 4ºC and plasma separated and frozen at -80ºC until analysis. Endogenous plasma vascular endothelial growth factor (VEGF) was quantified using a VEGF EIA Kit (R&D systems Europe, United Kingdom) accordingly to manufacturer's instructions. Absorbance was measured at 450 nm, with the correction wavelength set at 570 nm, using an ELISA plate reader (Perkin-Elmer, Wellesley, Massachusetts). A standard logarithmic curve was plotted and used to calculate VEGF concentrations in the plasma samples.

Quantitative real-time RT-PCR analysis

Two-step real-time RT-PCR was performed as previously described [19] using samples from right and left ventricles. Briefly, after total mRNA extraction using a commercial kit (no. 74124; Qiagen), standard curves were obtained for each gene correlating ($R>0.98$) the mRNA quantities in graded dilutions from a randomly selected tissue sample with the respective threshold cycles (second derivative maximum method). Equal amounts of mRNA from every sample underwent two-step real-time RT-PCR experiments for each gene, using SYBR green as marker (no. 204143; Qiagen).

GAPDH was used as internal control because its mRNA levels were similar between groups. Results are relative to the mean obtained for the NS group (set as arbitrary unit) after normalizing for GAPDH. Specific PCR primer pairs for the studied genes were: GAPDH: fw 5'- TGG CCT TCC GTG TTC CTA CCC -3' and rev 5'- CCG CCT GCT TCA CCA CCT TCT -3'; type-B natriuretic peptide (BNP) – fw 5'- CAG AGC TGG GGA AAG AAG AG -3' and rev 5'- GGA CCA AGG CCC TAC AAA AGA -3'; VEGF: fw 5' - GTA CCT CCA CCA TGC CAA GT - 3' and rev 5' - GCA TTA GGG GCA CAC AGG AC - 3'; VEGF-receptor 1 (VEGF-R1): fw 5' - CGG CAG ACC AAT ACA ATC CT - 3'and rev 5'- TGT ATT GAG GTC CGT GGT GA - 3'; VEGF-receptor 2 (VEGF-R2): fw 5' - ACA GTT CCC AGA GTG GTT GG - 3' and rev 5'- GTC ACT GAC AGA GGC GAT GA - 3'; Hypoxia-inducible factor-α (HIF-1α): fw 5' - TCA TAG GCG GTT TCT TGT AGC - 3' and rev 5' - CTA ACA AGC CGG GGG AGG AC - 3'; Sarcoplasmic reticulum Ca^{2+} ATPase (SERCA2a): fw 5' - AAT TCT AAT ACG ACT CAC TAT AGG GAG AAG GGG AGG AGA TGA GGT AGC GGA TGA A - 3' and rev 5' - CGA GTT GAA CCT TCC CAC AA - 3' and Phospholamban (PLB): fw 5' - AAT TCT AAT ACG ACT CAC TAT AGG GAG AAG GGG TGG - 3' and rev 5' - GGC ATC ATG GAA AAA GTC CA - 3'.

Statistical Analysis

Means and standard errors of mean were calculated for all variables in each group. Two-way ANOVA followed by the Bonferroni post-hoc test was used to compare groups. Statistical Package for the Social Sciences (SPSS Inc, version 10.0) was used for all analyses. The significance level was set at 5%.

Results

Characterization of the animals from the different groups

Animal data from the first and second set of animals (n=80) were pooled together for analysis. As seen in Table I, in comparison with NS, significantly lower body mass were

observed in NE, HS and HE. Moreover, body mass and femur length/body mass in the HE group were even lower that in HS. No differences were found concerning heart mass; however heart mass/body mass ratio was higher in NE and HE when compared to NS. As expected, hemoglobin concentration and hematocrit were significantly elevated in the hypoxic groups (HS and HE) when compared to their normoxic counterparts (NS and NE).

***** Insert Table I here *****

Heart mitochondrial bioenergetics

Table II shows the mitochondrial oxygen consumption endpoints for the different experimental groups. Respiration was sustained by using complex I (glutamate/malate) and II (succinate). A significant decrease in state 3 respiration with glutamate/malate was found in HE when compared to NE. In addition, state 4 respiration with both substrates decreased significantly in mitochondria from hypoxic groups (HS and HE) compared to their normoxic counterparts. RCR increased in NE, HS and HE mitochondria compared to NS when complex I substrates were used. Differences in the ADP/O ratio were found in succinate-energized mitochondria from hypoxic groups (HS and HE) when compared to their normoxic counterparts (NS and NE).

Results from mitochondrial membrane potential measurements (Table III) revealed that ADP caused a significantly lower membrane depolarization in NE and HE mitochondria energized with complex I substrates when compared with NS, the same occurring with the repolarization potential. When using complex II substrates, the only difference between experimental groups was related with the lag phase. In fact, when the hypoxic stimuli and the ET were combined (HE), mitochondria demonstrated a shorter lag phase than the sedentary normoxic and hypoxic groups (NS and HS, respectively).

***** Insert Table II here *****

***** Insert Table III here *****

In order to analyze whether IHH and ET and the combination of both approaches contributed to alter mitochondrial function through the modulation of critical electron transport chain complexes, immunoblotts of specific OXPHOS subunits for complex I, II, III and V were performed (Figure 1). IHH *per se* induced a significant decrease in levels complex -I and -II subunits as compared to normoxic control group (HS vs. NS). Moreover, IHH plus ET regimen (HE) completely reverted the decreased amount of complex -I and -II subunits (HE vs. HS). No alterations between experimental groups were observed in complex III and V subunits.

***** Insert Figure 1 here *****

In vitro A/R stress is an appropriate strategy to investigate intrinsic mitochondrial defenses [15]. In order to find out which experimental group would resist more to A/R, oxygen consumption endpoints were measured before and after the deleterious stimulus (Table IV). With the exception of ADP/O ratio in all groups and state 4 in HE group, A/R affected overall heart mitochondrial bioenergetics. Considering RCR the best general measure of mitochondrial function in isolated mitochondria [20], it was of notice that both IHH and ET significantly attenuated the decrease in mitochondrial function caused by A/R stress (NE, HS and HE vs. NS). However, no further effect was observed in the RCR of HE when compared to HS and/or NE groups.

***** Insert Table IV here *****

In order to investigate specific alterations that would suggest differential modulation of cardiac content of ANT, a mitochondrial protein involved in the phosphorylated system,

immunoblotts were performed (Figure 2). IHH combined with ET (HE) induced a significant increase in the content of ANT compared to all other groups.

Heart mitochondrial SIRT3, which is involved in the regulation of mitochondrial metabolism and resistance to oxidative stress [21], was semi-quantified by Western Blotting. However, no differences were found between groups regarding this specific sirtuin (data not shown).

Assessment of cardiac function and structure

ET (NE and HE groups) significantly increased left ventricle IVSs (Figure 3A), ejection fraction (Figure 3B), maximal aortic outflow (Ao) velocity (Figure 3C) compared to their sedentary counterparts (NS and HS), while LV dimensions were maintained (LVDs: NS: 3.2±0.2 mm, NE: 3.0±0.3 mm, HS: 3.2±0.4 mm, HE: 3.0±0.2 mm; LVDd: NS: 7.0±0.1 mm, NE: 6.3±0.4 mm, HS: 6.6±0.3 mm, HE: 6.7±0.2 mm). Time of isovolumic relaxation (IVRT) decreased in NE and HE when compared to NS and HS groups (Figure 3G). Doppler imaging revealed that ET (NE and HE) increased myocardial velocity both during systole, as shown by Sm (Figure 3E) and in diastole, as shown by Am (Figure 3F) compared to sedentary animals (NS and HS), while peak myocardial early diastolic velocity (Em) did not change significantly (NS: 3.2±0.2 $m.s^{-1}$, NE: 3.0±0.3 $m.s^{-1}$, HS: 3.2±0.4 $m.s^{-1}$, HE: 3.0±0.2 $m.s^{-1}$).

IHH *per se* increased the ratio between mitral E wave velocity and peak myocardial early diastolic velocity (E/Em) (Figure 3D). Moreover, IHH increased the time of isovolumic contraction (IVCT) (Figure 3H) but decreased Sm (Figure 3E) and Ao (Figure 3C).

IHH animals submitted to additional ET (HE) significantly showed improved myocardial performance as evaluated by Tei index compared to HS (Figure 3I). No alterations were found in this parameter between HE and NE. Furthermore, ejection fraction, Sm and Am were completely normalized (Figure 3B, E and F). We additionally calculated total vascular peripheral resistance (PR) to evaluate whether the hemodynamic

assessment could reflect vascular changes. Indeed, there was a trend towards an increase of PR in HS (207.1±16.1 mmHg.min.l^{-1}) and a normalization of this value in the HE rats (169.0±23.0 mmHg.min.l^{-1} vs NS: 171.5±11.6 mmHg.min.l^{-1}).

***** Insert Figure 3 here *****

With respect to hemodynamic measurements we observed an increase in stroke volume in NE when compared to NS. Moreover, it increased even further in HE. Cardiac output rose significantly in HE rats (HE vs. all other groups) (Table V). In the right ventricle, IHH prolonged the relaxation time constant-Tau and, as expected, increased systolic pressures (Table V). ET did not cause any alteration in these parameters. The response of cardiac function to isovolumic contractions in terms of ESP and EDP percentage of increase from baseline was also evaluated. However, no differences between groups were observed in these conditions. Upon an isovolumic contraction, IHH groups showed a trend to develop a higher maximal systolic pressure but these values were not significant (p=0.12, Table V). Preload recruitable stroke work showed a slight tendency to increase in ET groups (Table V).

***** Insert table V here *****

Vascular endothelial growth factor (VEGF) plasma levels

IHH significantly increased VEGF plasma levels (NS: 29.6±5.0 pg.mL^{-1}, NE: 21.9±6.9 pg.mL^{-1}, HS: 49.0±11.7 pg.mL^{-1}, HE: 43.1±4.7 pg.mL^{-1}, p=0.05). However, no further increase in plasma VEGF content was found IHH when combined with ET.

Gene expression profile

As shown in Figure 4, BNP gene expression in the overloaded RV increased in HS compared to NS being completely normalized in HE rats. The ratio of SERCA2a/PLB

significantly decreased in the LV of both hypoxic groups (HS and HE) compared to their normoxic counterparts (NS and NE), but remained unaltered in the RV. Except for a significant increase observed in LV VEGF-R1 expression induced by IHH (NS: 1.00±0.10; NE: 1.29±0.28, HS: 1.42±0.18, HE: 1.73±0.34), disappointingly no other alterations were observed in the expression of angiogenesis-related markers such as HIF-1α (RV - NS: 1.00±0.08, NE: 1.01±0.14, HS: 1.41±0.47, HE: 1.22±0.22; LV - NS: 1.00±0.30, NE: 1.49±0.46, HS: 1.25±0.20, HE: 1.84±0.70), VEGF (RV - NS: 1.00±0.09, NE: 1.38±0.28, HS: 0.94±0.11, HE: 0.92±0.04; LV - NS: 1.00±0.10, NE: 0.98±0.08, HS: 0.81±0.09, HE: 0.84±0.12), VEGF-r1 (RV - NS: 1.00±0.12, NE: 1.34±0.10, HS: 0.97±0.15, HE: 1.17±0.20), and VEGF-r2 (RV - NS: 1.00±0.06, NE: 1.03±0.06, HS: 0.75±0.17, HE: 0.79±0.11; LV - NS: 1.00±0.09, NE: 0.66±0.14, HS: 1.04±0.17, HE: 0.83±0.17).

***** Insert Figure 4 here *****

Discussion

Overview of findings

Despite some controversy [22], it is generally accepted that chronic intermittent hypoxia models that resemble repeated severe and short duration hypoxia/reoxygenation cycles, of which obstructive sleep apnea syndrome is an example, induce extreme ROS-associated cardiac dysfunction [23, 24]. It is however important to notice that the present less severe and longer cycle-based model of IHH and ET are considered non-pharmacological approaches that positively increase heart tissue tolerance against major harmful consequences of cardiac deleterious events, such as ischemia-reperfusion or drug-induced dysfunction [1, 8] targeting mitochondrial bioenergetics and (dys)function [4, 14]. Therefore, the main goal of the present study was to ascertain whether IHH exposure plus an ET regimen amplify mitochondrial and cardiac stress defenses and improve cardiac function and mitochondrial bioenergetics. Data

obtained from *in vitro* analysis of mitochondrial function revealed that both IHH and ET improved *per se* several endpoints of heart mitochondrial bioenergetics. Also, combination of these two cardioprotective strategies translated into further improvements of cardiac function evaluated under basal conditions, such as the observed increase of cardiac output, systolic volume and normalization of the Tei index. As a result of IHH exposure, a tendency for cardiac function improvement under afterload, which mimics a cardiac response to acute stress conditions, was also observed.

Heart mitochondrial bioenergetics

Mitochondria are vital components in cellular energetic metabolism and in distinct intracellular signaling processes. In fact, mitochondria are involved in a myriad of complex signaling cascades, namely some regulating cell death vs. survival [25]. Therefore, assessing mitochondrial function is critical to understand the relevance of the impact of distinct physiological or pathological stimuli on cells homeostasis [20].

The mitochondrial RCR is strongly influenced by almost every functional aspect of oxidative phosphorylation and it has been considered the best general measure of mitochondrial function in isolated mitochondria [20]. Under basal conditions, with mitochondria energized with substrates for complex I, the higher RCR found in all groups compared to NS group suggest that mitochondria from IHH, ET and combined regimens improved their coupling between respiration and ATP synthesis (Table II). Results regarding ET are consistent with previous data from our group and others [26] and reinforce the idea that this non-pharmacological intervention positively modulate cardiac mitochondria to a higher level of metabolic coupling. On the other hand, Zhu et al. [14] did not find any alteration in basal heart mitochondrial RCR caused by IHH though when supplemental calcium was added to the medium a significant lower uncoupling of the respiratory control was observed in the hypoxic groups. In accordance, after submitting mitochondria to an *in vitro* stress test of A/R, we found

that RCR was significantly less affected in the hypoxic and/or trained than in the normoxic sedentary animals (Table IV). Taking together, data suggest that pre-condition interventions through IHH and/or ET improved cardiac mitochondrial function at baseline and also prevented stress-induced alterations; however an additional improvement or protection was not afforded by the combination of both stimuli. Considering that absolute respiration rate can give additional useful insights into the mechanism of mitochondrial (dys)function, we also analyzed respiration rates during state 3 and state 4. RCR encapsulates the main function of mitochondria, i.e., their ability to idle at a low rate yet respond to ADP by producing ATP at a high rate [20]; however basal (state 4) and phosphorylating (state 3) respiratory rates revealed that IHH and ET seem to influence the increased RCR by distinct bioenergetics mechanisms. IHH influenced RCR through a significant reduction in state 4, which can be explained by a decreasing inner membrane leakage of protons. ET *per se* (NE vs. NS) altered state 3 improving the ability of mitochondria to produce ATP at a higher rate as previously reported by our group [15, 21, 26, 27].

In line with data previously demonstrated by others [28, 29], IHH induced a significant global decrease of the OXPHOS subunits with the particular contribution of complex I and II (Figure 1). However, in contrast, an increase in the activity of OXPHOS complexes I and III was found by Zaobornyj et al. [30] in heart mitochondria of rats adapted to long-lasting high-altitude hypoxia (4,340 m, 84 days). Interestingly, our study also showed for the first time, that ET combined with IHH (HE) was able to completely revert the decrease observed in OXPHOS subunit complex I and II in the HS group. Considering that the decreased content of an electron transport chain component subunit could not apparently be interpreted as a beneficial mitochondrial alteration in the context of cardioprotection, some have suggested that this down-regulation via PKC-δ may contribute to cardioprotection through the stimulation of autophagy, with consequent elimination of damaged mitochondria when a decrease in

OXPHOS complex occurs [29]. Further work is needed in order to better clarify this topic.

Although IHH and ET *per se* did not modify ANT content (NE and HS vs. NS), the combination of both cardioprotective strategies induced a significant increase in the protein content (HE vs. all other groups) (Figure 2). The important role of ANT in mitochondrial bioenergetics as ADP/ATP nucleotide translocator may also contribute to the protective phenotype observed in some functional endpoints in HE group.

We also measured SIRT3 in the cardiac tissue. SIRT3 is emerging as key regulator of many cellular functions including metabolism, cell growth, apoptosis, and genetic control of ageing [21]. In the heart, SIRT3 has been found to block development of cardiac hypertrophy and protect cardiomyocytes from oxidative stress-mediated cell death. Moreover, evidence for SIRT3-dependent regulation of global mitochondrial function was reported [31]. In particular, it was proposed that the absence of SIRT3 resulted in a marked alteration of basal *in vivo* ATP levels and that SIRT3 can reversibly bind to and regulate the acetylation and activity of Complex I of the electron-transport chain. However, in contrast with data revealing increases in the expression of rat skeletal muscle SIRT3 (particularly in the oxidative soleus muscle) after 6 weeks of voluntary wheel running [32], we were unable to detect any alteration in the content of these proteins in heart mitochondria from ET rats. Moreover, IHH protocol was also ineffective regarding the stimulation of the SIRT3 expression.

Cardiac function

As previously described, cardiac pre-conditioning induced by IHH and ET has been associated with several mechanisms including attenuated infarct size, myocardial fibrosis and apoptosis, diminished ROS release, preservation of calcium homeostasis, modulation of mitoKATP channels, increased vascularization as well as anti-arrhythmic and antioxidant capacity [1, 3]. However, intrinsic cardiac function using pressure-

volume hemodynamics after pre-conditioning IHH when combined with another well-known protective strategy such as ET was yet never addressed.

To understand the concomitant expression of the molecular adaptations perpetrated by IHH and/or ET pre-conditioning regimens in the overall cardiac tissue function and also to ascertain whether mitochondrial-related alterations translate into simultaneous functional phenotypes, *in vivo* hemodynamic measurements, as well as echocardiographic analysis were performed. In line with data previously discussed at molecular level, pre-exposure to IHH combined with ET improved myocardial function. A notable and hitherto unreported finding is the fact that HE rats displayed an enhanced myocardial performance as demonstrated by Tei index normalization and an increase in cardiac output, and stroke volume while arterial elastance decreased suggesting that significant vascular alterations may be occurring simultaneously. Indeed, the increase in cardiac output without a raise in ESP suggests that the mechanical performance of the heart in the HE group might be improved. Furthermore, hypoxic rats presented increased levels of plasma VEGF, which suggests increased angiogenesis. The Tei index has proved to be a reliable method for the evaluation of LV systolic and diastolic performance, being independent from heart rate, age and, importantly, blood pressure [34]. More important is the fact that the Tei index presents the advantage to evaluate myocardial function independently of the vascular effects that IHH and/or ET may induce.

Considering the relevance of measuring cardiac function under peak stress conditions, sudden afterload elevations, more precisely, isovolumic contractions induced by transient ascending aortic occlusions (table V) were therefore performed to assess inotropic reserve and to evaluate cardiac response to acute stress conditions. During this assessment, HS and HE (but not NE) animals showed a small tendency to an increased inotropic response, possibly highlighting the pre-conditioning value of IHH under stressful conditions imposed by pathological stimuli. Moreover, at the end of baseline cardiac function assessment, we also performed volume overload of

approximately 30% of circulating volume. These results were similar between groups (data not shown).

Despite our effort to echocardiographically and hemodynamically analyze the pre-conditioning influence of IHH, ET and the synergistic effect of both interventions on cardiac function under baseline and acute stress conditions, we cannot rule out that a final ischemia-reperfusion protocol would uncover stronger cardiac functional differences between groups. Further studies are needed to address this relevant issue.

Conclusions

Our data indicated that both IHH and ET positively modulate heart mitochondria under basal conditions and that the combination of the two strategies may not afford addictive protection. Our data suggests that the alteration of mitochondrial capacity resulting from these IHH and ET are associated with a more resistant basal phenotype. Moreover, the observed mitochondrial benefits seem to translate into overall cardiac function such as increased cardiac output and normalization of the Tei index. Further studies are in fact needed in order to mechanistically understand whether the combination of these strategies afford cardioprotection against cardiac deleterious stimuli or pathophysiological conditions to the heart such as ischemia-reperfusion, hyperglycemia, hypercholesterolemia, and drug-induced dysfunction.

Acknowledgments

The authors would like to thank Sandra Mendes for her committed participation in animal care and treatment. JM (SFRH/BPD/66935/2009), IO-G (SFRH/BD/62352/2009), IA (SFRH/BD/61889/2009), EP (SFRH/BD/71149/2010), ACM (SFRH/BD/33892/2009), NM (SFRH/BD/66178 /2009) and AA (SFRH/BPD/4225/2007) are supported by grants from the Portuguese Foundation for Science and Technology (FCT). The present work was supported by a research grant from the FCT (PTDC-DES-113580-2009, to Antonio Ascensao), from IJUP (71/2010) to José Magalhães and

from Research Centre in Physical Activity, Health and Leisure (CIAFEL) I&D Unit (PEst-OE/SAU/UI0617/2011) and the Cardiovascular R&D Unit (FCT nr. 51/94).

The authors of this manuscript have certified that they comply with the Principles of Ethical Publishing in the International Journal of Cardiology [35].

References

[1] Ascensao A, Ferreira R, Magalhaes J. Exercise-induced cardioprotection - biochemical, morphological and functional evidence in whole tissue and isolated mitochondria. Int J Cardiol 2007;16-30.

[2] Ostadal B, Kolar F. Cardiac adaptation to chronic high-altitude hypoxia: beneficial and adverse effects. Respir Physiol Neurobiol 2007;2-3:224-36.

[3] Kavazis AN. Exercise preconditioning of the myocardium. Sports Med 2009;11:923-35.

[4] Ascensao A, Lumini-Oliveira J, Oliveira PJ, Magalhaes J. Mitochondria as a target for exercise-induced cardioprotection. Curr Drug Targets 2011;6:860-71.

[5] Ascensao A, Oliveira PJ, Magalhaes J. Exercise as a beneficial adjunct therapy during Doxorubicin treatment--role of mitochondria in cardioprotection. Int J Cardiol 2012;1:4-10.

[6] Brown DA, Chicco AJ, Jew KN, Johnson MS, Lynch JM, Watson PA, Moore RL. Cardioprotection afforded by chronic exercise is mediated by the sarcolemmal, and not the mitochondrial, isoform of the KATP channel in the rat. J Physiol 2005;Pt 3:913-24.

[7] Quindry JC, Schreiber L, Hosick P, Wrieden J, Irwin JM, Hoyt E. Mitochondrial KATP channel inhibition blunts arrhythmia protection in ischemic exercised hearts. Am J Physiol Heart Circ Physiol 2010;1:H175-83.

[8] Kolar F, Ostadal B. Molecular mechanisms of cardiac protection by adaptation to chronic hypoxia. Physiol Res 2004;S3-13.

[9] Kolar F, Jezkova J, Balkova P, Breh J, Neckar J, Novak F, Novakova O, Tomasova H, Srbova M, Ost'adal B, Wilhelm J, Herget J. Role of oxidative stress in PKC-delta upregulation and cardioprotection induced by chronic intermittent hypoxia. Am J Physiol Heart Circ Physiol 2007;1:H224-30.

[10] Ostadalova I, Ostadal B, Jarkovska D, Kolar F. Ischemic preconditioning in chronically hypoxic neonatal rat heart. Pediatr Res 2002;4:561-7.

[11] Neckar J, Szarszoi O, Koten L, Papousek F, Ost'adal B, Grover GJ, Kolar F. Effects of mitochondrial K(ATP) modulators on cardioprotection induced by chronic high altitude hypoxia in rats. Cardiovasc Res 2002;3:567-75.

[12] Zhu HF, Dong JW, Zhu WZ, Ding HL, Zhou ZN. ATP-dependent potassium channels involved in the cardiac protection induced by intermittent hypoxia against ischemia/reperfusion injury. Life Sci 2003;10:1275-87.

[13] Zhu WZ, Xie Y, Chen L, Yang HT, Zhou ZN. Intermittent high altitude hypoxia inhibits opening of mitochondrial permeability transition pores against reperfusion injury. J Mol Cell Cardiol 2006;1:96-106.

[14] Zhu WZ, Xie Y, Chen L, Yang HT, Zhou ZN. Intermittent high altitude hypoxia inhibits opening of mitochondrial permeability transition pores against reperfusion injury. Journal of molecular and cellular cardiology 2006;1:96-106.

[15] Ascensao A, Magalhaes J, Soares JM, Ferreira R, Neuparth MJ, Marques F, Oliveira PJ, Duarte JA. Endurance training limits the functional alterations of heart rat mitochondria submitted to in vitro anoxia-reoxygenation. Int J Cardiol 2006;2:169-78.

[16] Van Norman KH. The Biuret Reaction and the Cold Nitric Acid Test in the Recognition of Protein. Biochem J 1909;3-4:127-35.

[17] Estabrook R. Mitochondrial respiratory control and the polarographic measurement of ADP/O ratios. Methods Enzymol 1967;41-47.

[18] Lumini-Oliveira J, Magalhaes J, Pereira CV, Moreira AC, Oliveira PJ, Ascensao A. Endurance training reverts heart mitochondrial dysfunction, permeability transition and apoptotic signaling in long-term severe hyperglycemia. Mitochondrion 2011;1:54-63.

[19] Roncon-Albuquerque R, Jr., Moreira-Rodrigues M, Faria B, Ferreira AP, Cerqueira C, Lourenco AP, Pestana M, von Hafe P, Leite-Moreira AF. Attenuation of the cardiovascular and metabolic complications of obesity in CD14 knockout mice. Life Sci 2008;13-14:502-10.

[20] Brand MD, Nicholls DG. Assessing mitochondrial dysfunction in cells. Biochem J 2011;2:297-312.

[21] Verdin E, Hirschey MD, Finley LW, Haigis MC. Sirtuin regulation of mitochondria: energy production, apoptosis, and signaling. Trends in biochemical sciences 2010;12:669-75.

[22] Naghshin J, McGaffin KR, Witham WG, Mathier MA, Romano LC, Smith SH, Janczewski AM, Kirk JA, Shroff SG, O'Donnell CP. Chronic intermittent hypoxia increases left ventricular contractility in C57BL/6J mice. Journal of applied physiology 2009;3:787-93.

[23] Dempsey JA, Veasey SC, Morgan BJ, O'Donnell CP. Pathophysiology of sleep apnea. Physiol Rev 2010;1:47-112.

[24] Leung RS, Comondore VR, Ryan CM, Stevens D. Mechanisms of sleep-disordered breathing: causes and consequences. Pflugers Arch 2012;1:213-30.

[25] Camara AK, Bienengraeber M, Stowe DF. Mitochondrial approaches to protect against cardiac ischemia and reperfusion injury. Frontiers in physiology 2011;13.

[26] Ascensao A, Magalhaes J, Soares JM, Ferreira R, Neuparth MJ, Marques F, Oliveira PJ, Duarte JA. Moderate endurance training prevents doxorubicin-induced in vivo mitochondriopathy and reduces the development of cardiac apoptosis. Am J Physiol Heart Circ Physiol 2005;2:H722-31.

[27] Ascensao A, Ferreira R, Oliveira PJ, Magalhaes J. Effects of endurance training and acute Doxorubicin treatment on rat heart mitochondrial alterations induced by in vitro anoxia-reoxygenation. Cardiovasc Toxicol 2006;3-4:159-72.

[28] Nouette-Gaulain K, Malgat M, Rocher C, Savineau JP, Marthan R, Mazat JP, Sztark F. Time course of differential mitochondrial energy metabolism adaptation to chronic hypoxia in right and left ventricles. Cardiovascular research 2005;1:132-40.

[29] Hlavackova M, Kozichova K, Neckar J, Kolar F, Musters RJ, Novak F, Novakova O. Up-regulation and redistribution of protein kinase C-delta in chronically hypoxic heart. Molecular and cellular biochemistry 2010;1-2:271-82.

[30] Zaobornyj T, Valdez LB, Iglesias DE, Gasco M, Gonzales GF, Boveris A. Mitochondrial nitric oxide metabolism during rat heart adaptation to high altitude: effect of sildenafil, L-NAME, and L-arginine treatments. American journal of physiology. Heart and circulatory physiology 2009;6:H1741-7.

[31] Ahn BH, Kim HS, Song S, Lee IH, Liu J, Vassilopoulos A, Deng CX, Finkel T. A role for the mitochondrial deacetylase Sirt3 in regulating energy homeostasis. Proceedings of the National Academy of Sciences of the United States of America 2008;38:14447-52.

[32] Vainshtein A, Kazak L, Hood DA. Effects of endurance training on apoptotic susceptibility in striated muscle. Journal of applied physiology 2011;6:1638-45.

[33] Xu WQ, Yu Z, Xie Y, Huang GQ, Shu XH, Zhu Y, Zhou ZN, Yang HT. Therapeutic effect of intermittent hypobaric hypoxia on myocardial infarction in rats. Basic research in cardiology 2011;3:329-42.

[34] Lakoumentas JA, Panou FK, Kotseroglou VK, Aggeli KI, Harbis PK. The Tei index of myocardial performance: applications in cardiology. Hellenic J Cardiol 2005;1:52-8.

[35] Shewan LG, Coats AJS. Ethics in the authorship and publishing of scientific articles. Int J Cardiol 2010;1-2.

Figure legends

Figure 1. Effects of IHH and/or ET on heart mitochondrial electron transport chain complex subunits Complex I NDUFB8 (20 kDa, A), Complex II Fe-S (30 kDa, B), Complex III core 2 (47 kDa, C) and ATP synthase alpha 53 kDa subunit (D). Typical immunoblotts of the respective proteins are presented (lower panel). Experiments were performed for an n=6/group. Control for protein loading was confirmed by Ponceau-S staining. * vs. control NS ($p<0.05$). Data are mean ± SEM.

Figure 2. Effects of IHH and/or ET on heart mitochondrial ANT. Typical immunoblot of the protein is presented (lower panel). Experiments were performed for an n=6/group. Control for protein loading was confirmed by Ponceau-S staining. * vs. control NS ($p<0.05$). Data are mean ± SEM

Figure 3: Echocardiographic evaluation of the left ventricle performed 2 days before final hemodynamic instrumentation. Experiments were performed for an n=10/group. A) Interventricular septum thickness in systole (IVSs, mm); B) Ejection fraction (%); C) Maximal aortic outflow velocity (Ao, $m.s^{-1}$); D) Ratio between mitral E wave velocity and peak myocardial early diastolic velocity (E/Em); E) Peak myocardial systolic velocity (Sm, $m.s^{-1}$); F) Peak myocardial late diastolic velocity (Am, $m.s^{-1}$); G) Isovolumic relaxation time (IVRT, ms); H) Isovolumic contraction time (IVCT, ms); I) Tei index. ET significantly increased IVSs ($p=0.04$), EF ($p=0.03$), Sm ($p=0.02$), Am ($p=0.03$) and Ao ($p=0.04$). IHH increased E/Em ($p=0.01$, Figure 1G) and IVCT ($p=0.001$) while decreased Sm ($p=0.02$) and Ao ($p=0.02$). ET in hypoxic conditions normalized the Tei index. * vs. NS; $^{\$}$ vs. NE; $^{\#}$ vs. HS ($p<0.05$). Data are mean ± SEM.

Figure 4: Expression of type-B natriuretic peptide (BNP) and ratio between sarcoplasmic reticulum Ca^{2+} ATPase (SERCA2a) and phospholamban (PLB) in right (RV, A and C, respectively) and left ventricle (LV, B and D, respectively) collected after hemodynamic instrumentation. BNP results are normalized for GAPDH and expressed in arbitrary units (AU). Experiments were performed for an n=10/group. * vs. NS; $^{\$}$ vs. NE; $^{\#}$ vs. HS ($p<0.05$). Data are mean ± SEM.

Table I. Animal data and mitochondrial isolation yield

	NS	NE	HS	HE
Body mass (g)	393.1 ± 6.2	342.6 ± 7.1*	359.2 ± 8.2*	316.0 ± 9.1*,#
Heart mass (g)	0.84 ± 0.05	0.85 ± 0.04	0.88 ± 0.07	0.88 ± 0.02
Heart mass/body mass ($mg.g^{-1}$)	2.20 ± 0.10	2.44 ± 0.13*	2.47 ± 0.20	2.75 ± 0.11*
Femur length/body mass ($mm.g^{-1}$)	0.093 ± 0.001	0.104 ± 0.002*	0.112 ± 0.002*	0.094 ± 0.004#
Hemoglobin ($g.dl^{-1}$)	14.30 ± 0.30	14.37 ± 0.15	21.03 ± 0.72*	18.91 ± 0.10*,$
Hematocrit (%)	43.24 ± 1.27	43.17 ± 0.38	64.75 ± 3.31*	58.26 ± 0.36*,$
Heart mitochondrial isolation yield ($mg.g^{-1}$)	19.6 ± 2.0	23.4 ± 3.5	21.0 ± 0.8	21.7 ± 1.7

Data are mean ± SEM. NS, normoxic sedentary; NE, normoxic exercised; HS, hypoxic sedentary; HE, hypoxic exercised. * vs. NS, # vs. HS, $ vs. NE, $p<0.05$

Table II. Effect of IHH and/or ET on state 3 and state 4 respiratory rates and on RCR and ADP/O ratios of rat heart mitochondria energized with substrates for complex I and for complex II

	State 3	State 4	RCR	ADP/O
	nmolatmsO/mg prot/min	nmolatmsO/mg prot/min		
	Complex I (glutamate/malate)			
NS	451.8 ± 28.2	70.6 ± 2.2	6.4 ± 0.3	2.6 ± 0.2
NE	507.5 ± 23.1	68.3 ± 1.9	7.4 ± 0.4*	3.4 ± 0.3
HS	429.0 ± 34.2	56.0 ± 3.8*	7.8 ± 0.1*	3.6 ± 0.3
HE	403.8 ± 14.2$^{\$}$	53.3 ± 2.6*,$^{\$}$	7.6 ± 0.3*	3.4 ± 0.5
	Complex II (succinate)			
NS	568.1 ± 58.2	213.1 ± 10.2	2.6 ± 0.2	2.0 ± 0.2
NE	521.2 ± 86.0	189.0 ± 15.1	2.7 ± 0.3	1.8 ± 0.2
HS	524.9 ± 71.9	173.2 ± 9.8*	3.1 ± 0.4	3.0 ± 0.1*
HE	591.1 ± 75.8	175.2 ± 8.8*,$^{\$}$	3.3 ± 0.3	3.0 ± 0.3*,$^{\$}$

Data are mean ± SEM for heart mitochondria (0.5 mg/mL protein) isolated from all experimental groups and obtained from 10 independent isolations from each group. Oxidative phosphorylation was measured polarographically at 25ºC in a total volume of 0.75 mL. Respiration medium and other experimental details are provided in the materials and methods section. RCR – respiratory control ratio (state 3/state 4); ADP/O - number of nmol ADP phosphorylated by natoms O consumed; NS, normoxic sedentary; NE, normoxic exercised; HS, hypoxic sedentary; HE, hypoxic exercised; * vs. NS; $^{\$}$ vs. NE, $p<0.05$

Table III. Effect of IHH and/or ET on electric transmembrane potential (ΔΨ) fluctuations of rat heart mitochondria energized with complex I and II substrates

	Initial Polarization	ADP Depolarization	Repolarization	Lag Phase
		ΔΨ (*-mV*)		*s*
	Complex I (glutamate plus malate)			
NS	219.5 ± 1.9	185.0 ± 2.1	216.9 ± 1.7	48.8 ± 2.7
NE	214. ± 1.8	175.9 ± 2.9*	209.1 ± 1.3*	49.2 ± 6.4
HS	218.9 ± 2.8	178.5 ± 3.1	214.5 ± 2.4	50.7 ± 5.7
HE	215.9 ± 2.3	176.2 ± 1.7*	210.4 ± 1.9*	53.1 ± 6.5
	Complex II (succinate)			
NS	223.6 ± 2.7	182.1 ± 2.3	221.7 ± 2.2	51.4 ± 1.6
NE	219.4 ± 5.2	181.4 ± 1.7	216.9 ± 3.2	43.8 ± 2.7
HS	222.0 ± 1.7	178.4 ± 2.5	221.0 ± 1.8	48.8 ± 2.9
HE	218.0 ± 2.4	178.6 ± 3.9	218.2 ± 2.9	37.2 ± 6.2*,#

Data are means ± SEM for heart mitochondria (0.5 mg/mL protein) isolated from all experimental groups and obtained from 10 independent isolations. Table shows the values for mitochondrial transmembrane potential developed with glutamate (10 mM) plus malate (5 mM) and with sucinate (2 mM) plus rotenone (4 μM), the decrease in transmembrane potential after ADP addition (depolarization), the repolarization value after ADP phosphorylation, and the lag phase that precedes repolarization. Mitochondrial transmembrane potential was measured using a TPP^+-selective electrode at 25ºC in a total volume of 1 mL. Reaction medium and other experimental details are provided in the methods section; NS, normoxic sedentary; NE, normoxic exercised; HS, hypoxic sedentary; HE, hypoxic exercised; * vs. NS; # vs. HS, $p<0.05$

Table IV. Effect of anoxia-reoxigenation (A/R) on the respiratory rates of heart mitochondria energized with substrates for complex I

	State 3 nmolatmsO/mg prot/min		State 4 nmolatmsO/mg prot/min		RCR		ADP/O	
	Before A/R	**After A/R**	**Before A/R**	**After A/R**	**Before A/R**	**After A/R**	**Before A/R**	**After A/R**
NS	451.8 ± 28.2	156.7 ± 4.8[a] (189%)	70.6 ± 2.2	91.4 ± 2.6 [a] (23%)	6.4 ± 0.3	1.7 ± 0.1 [a] (276%)	2.6 ± 0.2	2.5 ± 0.2 (4%)
NE	507.5 ± 23.1	176.9 ± 13.9[a] (186%)	68.3 ± 1.9	78.3 ± 1.9* [a] (13%)	7.4 ± 0.4*	2.3 ± 0.2* [a] (221%)	3.4 ± 0.3	2.9 ± 0.5 (17%)
HS	428.9 ± 34.2	194.6 ± 5.3* [a] (121%)	56.0 ± 3.8*	72.3 ± 7.1 [a] (22%)	7.8 ± 0.1*	2.7 ± 0.1* [a] (188%)	3.6 ± 0.3	3.1 ± 0.4 (16%)
HE	403.8 ± 14.2[$]	147.1 ± 8.5[#,$ a] (174%)	53.3 ± 2.6[$]	57.9 ± 3.3*[,#,$] (9%)	7.6 ± 0.3*	2.6 ± 0.1* [a] (192%)	3.4 ± 0.5	3.1 ± 0.5 (10%)

Data are mean±SEM for heart mitochondria (0.5 mg/mL protein) isolated from all experimental groups and obtained from 10 independent experiments. Oxidative phosphorylation was measured polarographically at 25ºC in a total volume of 0.75 mL. Respiration medium and other experimental details are provided in methods. RCR – respiratory control ratio (state 3/state 4); ADP/O - number of nmol ADP phosphorylated by nanomoles O_2 consumed. NS, normoxic sedentary; NE, normoxic exercised; HS, hypoxic sedentary; HE, hypoxic exercised. * vs. NS, [#] vs. HS, [$] vs. NE, [a] vs. Before A/R, $p<0.05$, (% - percentage of variation before *vs.* after A/R).

Table V. Effect of IHH and/or ET on hemodynamic parameters

	NS	NE	HS	HE
Baseline				
HR (bpm)	330±28	330±67	354±22	310±25
CO ($mL.min^{-1}$)	46.2±4.5	49.3±8.0	46.7±2.7	62.3±2.9*$#
SV (µl)	143.0±14.1	160.2±9.6*	131.7±11.8	172.4±26.7#
PR ($mmHg.min.l^{-1}$)	171.5±11.6	185.1±41.6	207.1±16.2	169.0±23.0
RV Function				
ESP (mmHg)	25.0±1.1	25.6±2.0	32.8±1.3*	31.5±3.8$
EDP (mmHg)	3.3±0.5	3.5±0.2	3.8±0.3	4.1±0.5
dP/dt_{max} ($mmHg.s^{-1}$)	2049±151	2313±225	2370±227	2413±470
dP/dt_{min} ($mmHg.s^{-1}$)	-1336±141	-1634±396	-1464±70	-1335±304
Tau (ms)	14.4±3.4	11.0±3.7	25.0±6.5*	22.3±5.6$
LV Function				
ESP (mmHg)	95.1±9.9	116.9±17.7	112.6±5.8	107.2±15.4
EDP (mmHg)	5.2±0.8	5.9±1.7	4.5±0.7	5.0±0.6
dP/dt_{max} ($mmHg.s^{-1}$)	7279±1084	10053±1351	8400±854	9347±2010
dP/dt_{min} ($mmHg.s^{-1}$)	-6418±1500	-6876±629	-6584±500	-5526±1199
Tau (ms)	15.3±2.1	13.6±0.6	15.6±1.1	16.7±1.1
E_A ($mmHg.µl^{-1}$)	0.65±0.10	0.56±0.12	0.81±0.07	0.56±0.01#
IVC Occlusions				
LV-ESPVR ($mmHg.µl^{-1}$)	32.2±10.4	32.6±15.7	41.1±19.2	39.7±25.8
LV-PRSW (mmHg)	52.3±13.8	96.5±26.5	52.1±10.8	76.0±17.3
LV-EDPVR ($mmHg.µl^{-1}$)	0.06±0.01	0.10±0.03	0.17±0.09	0.13±0.07
AA Occlusions				
Isovolumic contraction (Δ% baseline)	151.3±20.9	142.5±34.3	184.7±44.4	197.4±33.1

Data are mean ± SEM. AA, ascending aorta; CO, cardiac output; dP/dt_{max}, maximal rate of pressure rise; dP/dt_{min}, maximal rate of pressure decline E_A, arterial elastance; EF, ejection fraction; HR, heart rate; IVC, inferior vena cava; EDP, end-diastolic pressure; ESP, end-systolic or maximum pressure; EDPVR, end-diastolic pressure-volume relationship slope; ESPVR, end-systolic pressure-volume relationship slope; LV, left ventricle; RV, right ventricle; PR, vascular peripheral resistance; PRSW, preload recruitable stroke work slope and Tau, time-constant of isovolumic relaxation calculated by glantz method. * $p<0.05$ vs. NS; $ $p<0.05$ vs. NE; # $p<0.05$ vs. HS.

Figure 1

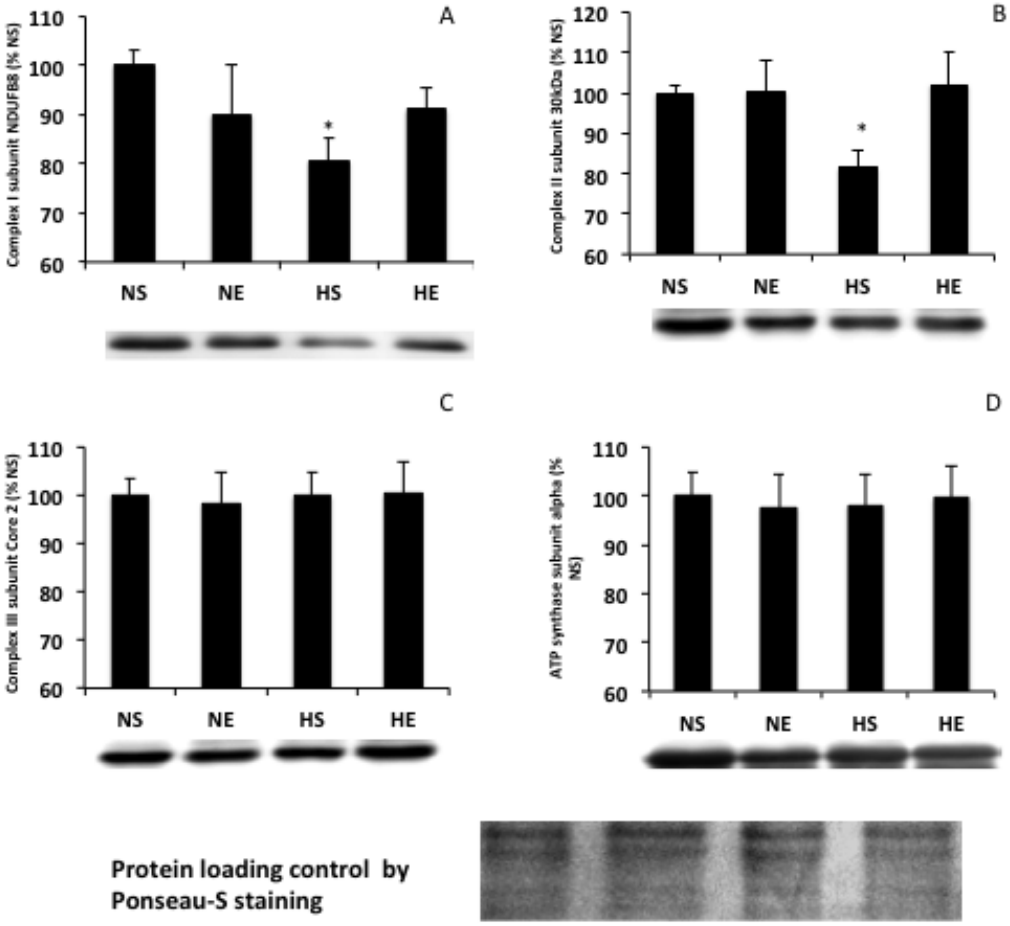

Figure 2

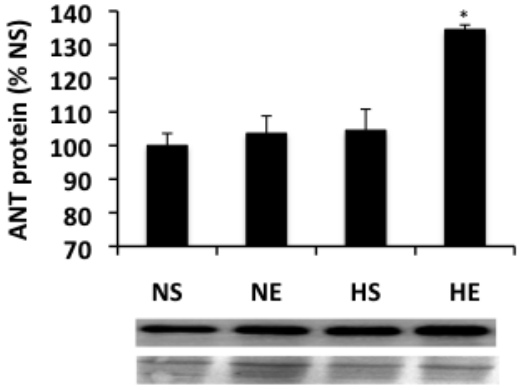

Figure 3

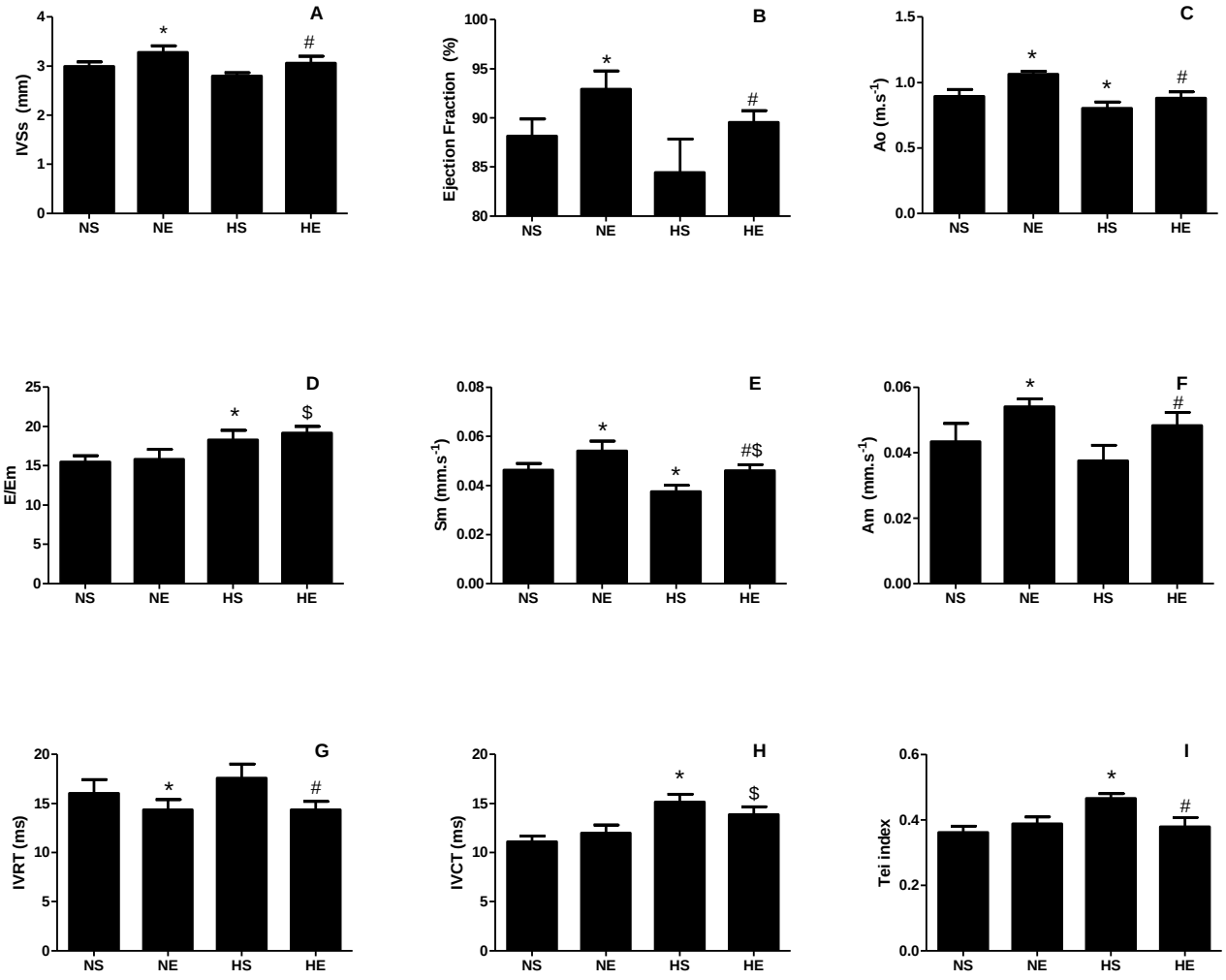

Figure 4